

Time arrival structures of the empirical Green's function extracted from ambient noise in shallow water

Xishan Yang⁽¹⁾⁽²⁾, Fenghua Li⁽¹⁾

⁽¹⁾State Key Laboratory of Acoustics, Institute of Acoustics, Chinese Academy of Sciences, Beijing, 100190, China.
oucyxs@163.com,

⁽²⁾University of Chinese Academy of Sciences, Beijing, 100049, China. lfh@mails.ioa.ac.cn

Abstract

Theoretical and experimental results show that the empirical Green's function (EGF) can be extracted by correlating the ambient noise between two sensors. Ambient noise was recorded continuously on two horizontal line arrays (HLAs) deployed in shallow water with horizontal separations of approximately 0.5 km. Stable EGFs (20–400 Hz) were extracted from ambient noise correlations between the HLAs using array beamforming which can accelerate the convergence rate of EFGs significantly. The EGFs extracted from the short-distance arrays have three distinct envelopes which correspond the head wave, the direct wave and the surface-reflected wave. The fluctuations of travel times of EGFs are shown to be in agreement with the variations of sound speed files. It is helpful in developing passive acoustic tomography systems. .

Keywords: Noise correlations, Arrival structures, Green's function

1 INTRODUCTION

It has been demonstrated that the cross-correlation function of the Brownian noise at two positions yields the arrival-time peaks as though there were an acoustic source at one position and a receiver at the other position within a diffuse ultrasonic field.[10] The same theory of correlating the random signals to extract their coherent aspects has been applied theoretically and experimentally to both land seismic[7] and ocean environments[8]. The time derivative of the correlations leads to an approximation of the empirical Green's function(EFG) between the sensor points, which provides an alternative possibility for monitoring the ocean environment. The surface reflected ray paths have been obtained the local Green's function on a horizontal array with a length of about 120m.[4] The critical angle can be extracted from the strength of the surface reflected ray paths. The deterministic normal modes have also been retrieved from cross-correlations of acoustic noise on three moored near-bottom instruments with horizontal separations of approximately 5km, 10km. [1]

In the ocean, though, the constantly changing environment means that the propagation path could change before the correlation reaches stochastic convergence. To enhance the emergence rate of EGFs, researchers have implemented the beam-forming technique on a vertical array[9] and on two separated arrays[9, 5]. Our study will show the improvement on the extraction rate of the EFGs from two horizontal arrays by beamforming technique. The time arrival structures of the EFGs are analyzed and the different ray paths of the EFGs are expected to be used in the passive acoustic tomography.

This paper is organized as follows. Section 2 presents a generalized theoretical formulation for the Green's function extraction with conventional beam-forming. Section 3 investigates the time arrival structures of the EFGs extracted from ocean ambient noise in shallow water. The conclusions are summarized in Section 4.



2 THEORY

The cross-correlation of the signals received at two separate sensors (the m th hydrophone of array A and the n th hydrophone of array B, as shown in Fig. 1), is given by

$$C_{m,n}(\tau) = \int_{-T_r/2}^{T_r/2} p(\mathbf{r}_{A,m}, t + \tau) p(\mathbf{r}_{B,n}, t) dt, \quad (1)$$

where T_r is the recording duration, $\mathbf{r}_{A,m}$ and $\mathbf{r}_{B,n}$ are the locations of the two sensors, and $p(\mathbf{r};t)$ is the pressure field recorded at each sensor. In the frequency domain, Eq. (1) becomes

$$C_{m,n}(\omega) = \frac{1}{T_r} p(\mathbf{r}_{A,m}, \omega) p^*(\mathbf{r}_{B,n}, \omega), \quad (2)$$

where $p^*(\mathbf{r}_{B,n}, \omega)$ is the complex conjugate of $p(\mathbf{r}_{B,n}, \omega)$, and ω is the angular frequency. The time derivative of the NCF has been proved to be approximately the sum of time-domain EGFs[11]:

$$\frac{dC_{m,n}(\tau)}{d\tau} \approx -G(\mathbf{r}_{A,m}, \mathbf{r}_{B,n}; \tau) + G(\mathbf{r}_{B,n}, \mathbf{r}_{A,m}; -\tau), \quad (3)$$

where $G(\mathbf{r}_{A,m}, \mathbf{r}_{B,n}; \tau)$ is the causal EGF located at $\mathbf{r}_{A,m}$ transmitting to $\mathbf{r}_{B,n}$, $G(\mathbf{r}_{B,n}, \mathbf{r}_{A,m}; -\tau)$ is the acausal EGF transmitting from $\mathbf{r}_{B,n}$ to $\mathbf{r}_{A,m}$, and τ is the time delay between the two receivers.

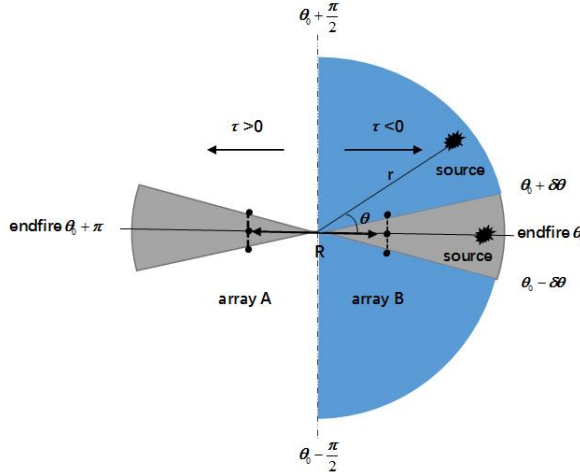


Figure 1. (Color online) Definition of the geometric variables for waves that travel from different directions to two receiver arrays. The regions of constructive interference are indicated by gray, and the blue regions correspond to the noise at the sides where $\tau < 0$.

To improve the convergence of the cross-correlation function, the signals from two arrays of hydrophones can be beam-formed and used in place of the signals from the two individual sensors. Now, it is assumed that $\theta = \theta_0$ is one of the end-fire directions of the m th hydrophone of array A and the n th hydrophone of array B, as shown in Fig. 1. When the array is not very long, the plane wave beam on array A in the end-fire direction of $\theta = \theta_0$ can be expressed as

$$b_A(\theta_0) = \mathbf{w}_A^H(\theta_0) \mathbf{p}_A, \quad (4)$$

where $\mathbf{w}_A(\theta_0) = [w_{A1}(\theta_0), w_{A1}(\theta_0), \dots, w_{AM}(\theta_0)]^T$ is the weight vector of array A, with $w_{Am}(\theta_0) = \exp(-i\omega\tau_m(\theta_0))$. For simplicity and clarity, the regular frequency ω has been omitted. Here, $(\bullet)^H$ denotes a complex transpose operation, $(\bullet)^T$ is a transpose operation, $\mathbf{p}_A = [p(\mathbf{r}_{A,1}), p(\mathbf{r}_{A,2}), \dots, p(\mathbf{r}_{A,M})]^T$ is the frequency-domain signal received by array A, and M is the number of array elements. Similarly, the plane wave beam on array B is denoted by $b_B(\theta_0)$. The cross-correlation function between the beams of array A and array B in the direction θ_0 is

$$C_{AB}(\theta_0) = b_A(\theta_0)b_B^H(\theta_0) = \mathbf{w}_A^H(\theta_0)\mathbf{p}_A\mathbf{p}_B^H\mathbf{w}_B(\theta_0). \quad (5)$$

With the beam-forming technique, the end-fire direction signals beneficial for extraction are not affected, but the signals from non-end-fire directions are filtered out. One can obtain $20\log_{10}\sqrt{MN}$ array gain in ideal conditions,[2] which means the emergence rate of extraction will be enhanced significantly.

3 EXPERIMENT

3.1 Overview of experiment

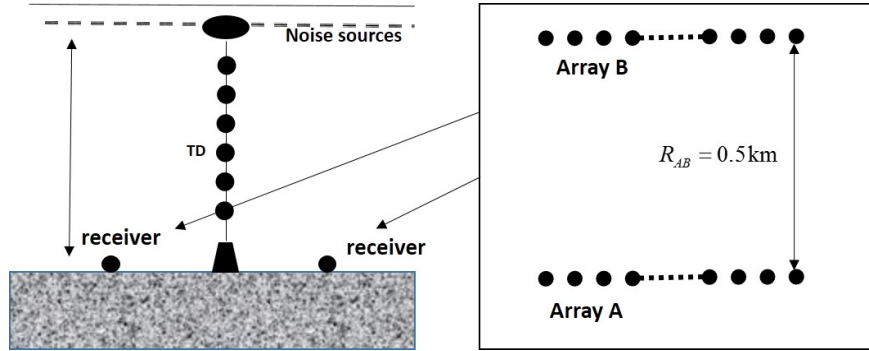


Figure 2. Schematic of the layout of the experiment site and the two bottom horizontal arrays. Arrays A and B are approximately parallel to each other. A vertical thermistor chain was placed between arrays A and B to acquire sound speed profiles.

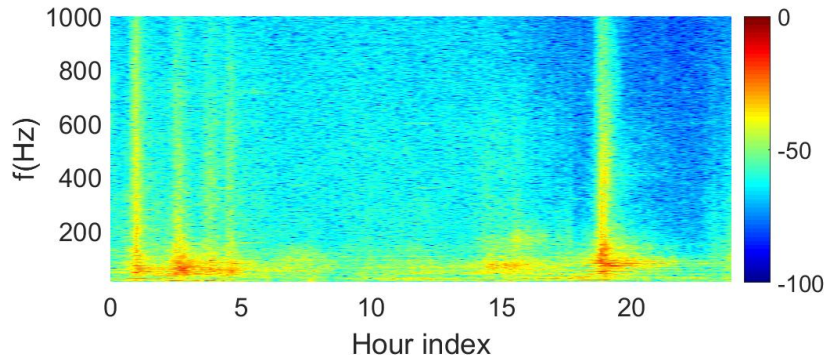


Figure 3. (Color online) Spectrogram of the ambient noise recorded over 24 h in the frequency band [10–1000 Hz]. The maximum value was set to unity (i.e., 0 dB).

The experiment was carried out in the South China Sea in 2018. Two self-recorded separated horizontal arrays, arrays A and B positioned as shown in Fig. 2, were deployed on the bottom to collect noise signals in shallow

water. The distance between arrays A and B is about 0.5 km. The two arrays are approximately parallel to each other. A thermistor chain was used to achieve water column sound speed profiles (SSPs) during the experiment for some time periods. Other technical features of the environment parameters have been described previously.[3]

A typical normalized noise spectrum is shown in Fig. 3. The noise spectrum changes considerably and it indicates that the ocean noise is highly non-stationary. The ambient noise level appears to be significantly higher in the low-frequency band ($f < 200$ Hz) for most of the 24 h. At low frequencies, the ambient noise field is primarily dominated by shipping noise.

3.2 Experimental results

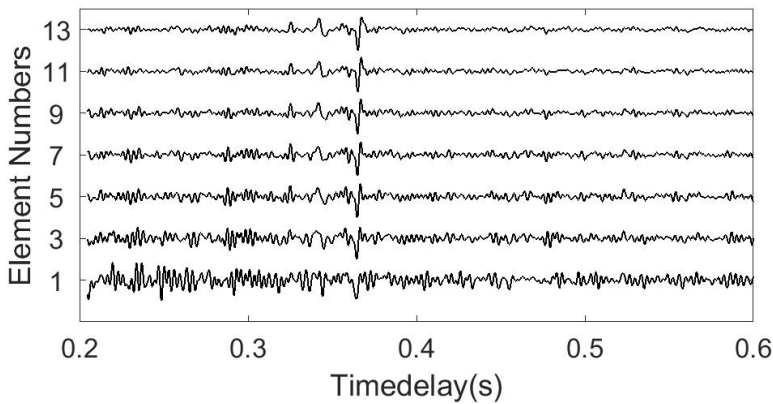


Figure 4. Envelope of EGFs extracted from different element numbers for an accumulation time of 24 h.

Here, arrays A and B were used to extract the EGFs between them. 24 hours of ambient noise was segmented into consecutive short intervals, each of duration 10 s. Prior to computing the cross-correlation functions, each 10 s of recorded data was filtered in the dominant frequency band (20–400 Hz).

Figure 4 compares the EGFs obtained by two hydrophones and two arrays for different element numbers. It can be seen from the figure that the beamforming technique significantly improve the rate of EGFs extraction from ocean ambient noise.

The time-domain of the EFG between the two short-distance is shown as the black line in Fig. 5a. From the figure, it can be seen that the signal contains three envelopes. At the same time, the ray-based Bellhop simulation was calculated for 210 Hz, which is the center frequency of 20–400 Hz. The arrival-time structure of the ray-based simulation is also shown by solid line in Fig. 5b. It can be found that the second peak corresponds to the direct path. The third peak corresponds to the eigenray striking the sea surface once.

From the simulation, it can be found that the first peak of the extracted signal does not relate to any eigenray in water column. From its arrival time, it can be obtained that the sound speed of the first envelope is about 1610 m/s, which is almost equal to the sediment sound speed in the experimental area. It is known that oceanic sources can cause head waves at the water-sediment interface. Consider a point source that produces a spherically spreading wave in a simple waveguide. Inside the critical range, where the incident ray is above the critical angle, the direct wave splits into reflected and transmitted waves.[6] Beyond the critical range, the direct wave is totally reflected. However, at the critical range, where the incident ray is exactly at the critical angle, the transmitted wave travels parallel to the interface. This part of the transmitted wave is the so-called lateral wave.

In the EGFs extraction, one correlates noise signals between two receivers by averaging over a sufficiently long time, and then only the noise sources propagating through both receivers contribute to the EGFs. Thus, the

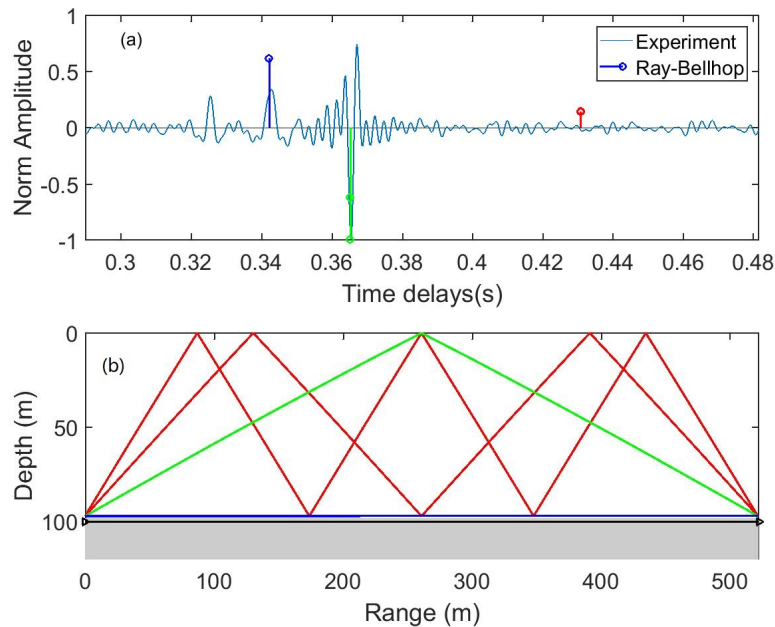


Figure 5. (Color online) (a) Comparison of ray-based time arrivals (colorful stem pattern) of Green's function with the EFG extracted from experiments (blue line). (b) Ray-based simulated eigenrays corresponding to the ray paths in (a), and the black line represents the head wave.

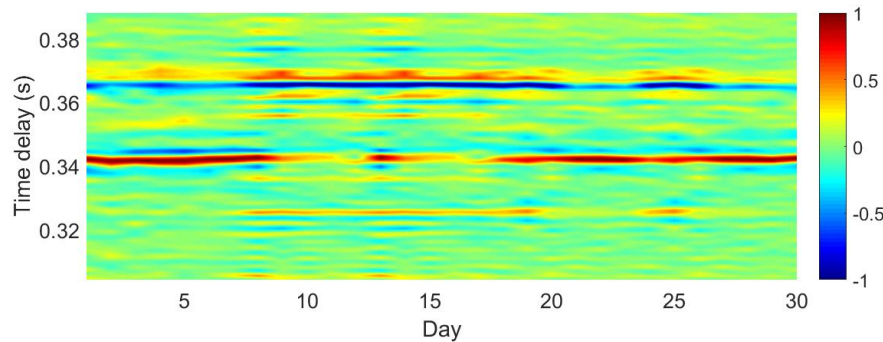


Figure 6. (Color online) Time-domain EGFs extracted from ambient noise between arrays A and B by beam-forming every 24 h for 30 days. The maximum amplitude in each signal was set to 1.

first envelope comes from lateral waves transmitting through two arrays in sediments. After correlating the noise, these lateral waves become a head wave in the extracted EFG. The sediment sound speed, which plays a significant role in the sound propagation, can be inverted directly.

Figure 6 shows the experimental EFGs every 24 h for 30 days. From the figure, it can be seen that the arrival times of head waves are constant over time. However, the arrival times of the second and third envelopes fluctuate with different time due to the change of the SSPs in water column.

4 CONCLUSIONS

The use of beamforming technique dramatically improves the strength of the correlated signal and reduces the time needed to build up the signal peak when correlating ambient noise recorded at horizontally separated sensors. Stable EFGs (20–400 Hz) were extracted from the ambient noise correlations from three arrays for about five months certificate the robustness of this methods. Head waves, which can be used to invert the sediment sound speed, were obtained from the EFGs between two short-distance arrays. The arrival time fluctuations of the EFGs extracted from two long-distance arrays can be used to conduct the passive tomography.

ACKNOWLEDGEMENTS

This research was supported by the National Natural Science Foundation of China under Grant Nos.11874061 and 11434012.

REFERENCES

- [1] M. G. Brown, O. A. Godin, N. J. Williams, N. A. Zabotin, L. Zabotina, and G. J. Bunker. Acoustic green's function extraction from ambient noise in a coastal ocean environment. *Geophysical Research Letters*, 41(15):5555–5562, 2015.
- [2] L. Charlotte, L. Shane, K. G. Sabra, W. S. Hodgkiss, W. A. Kuperman, and R. Philippe. Enhancing the emergence rate of coherent wavefronts from ocean ambient noise correlations using spatio-temporal filters. *Journal of the Acoustical Society of America*, 132(2):883–93, 2012.
- [3] Y. Z. W. L. W. G. Fenghua Li, Xishan Yang. Passive ocean acoustic tomography in shallow water. *Journal of the Acoustical Society of America*, 145(5):2823–2830, 2019.
- [4] S. E. Fried, W. A. Kuperman, K. G. Sabra, and R. Philippe. Extracting the local green's function on a horizontal array from ambient ocean noise. *Journal of the Acoustical Society of America*, 124(4):EL183–EL188, 2008.
- [5] S. E. Fried, S. C. Walker, W. S. Hodgkiss, and W. A. Kuperman. Measuring the effect of ambient noise directionality and split-beam processing on the convergence of the cross-correlation function. *Journal of the Acoustical Society of America*, 134(3):1824–32, 2013.
- [6] J. Gebbie and M. Siderius. Head wave correlations in ambient noise. *Journal of the Acoustical Society of America*, 140(1):EL62, 2016.
- [7] C. Michel and P. Anne. Long-range correlations in the diffuse seismic coda. *Science*, 299(5606):547–549, 2003.
- [8] P. Roux and W. A. Kuperman. Extracting coherent wave fronts from acoustic ambient noise in the ocean. *The Journal of the Acoustical Society of America*, 116(4):1995–2003, 2004.
- [9] M. Siderius, C. H. Harrison, and M. B. Porter. A passive fathometer technique for imaging seabed layering using ambient noise. *Journal of the Acoustical Society of America*, 120(120):1315–1323, 2006.

- [10] R. L. Weaver and O. I. Lobkis. Ultrasonics without a source: thermal fluctuation correlations at mhz frequencies. *Physical Review Letters*, 87(13):134301, 2001.
- [11] Z. Xiaoqin, M. G. Brown, and O. A. Godin. Waveform modeling and inversion of ambient noise cross-correlation functions in a coastal ocean environment. *Journal of the Acoustical Society of America*, 138(3):1325, 2015.